arXiv:1407.6021v2 [cond-mat.mes-hall] 29 Aug 2014

Quasiparticle renormalization in ABC graphene trilayers

Xu Dou,[1] Akbar Jaefari,[1] Yafis Barlas,[2] and Bruno Uchoa[1]

[1] *Department of Physics and Astronomy, University of Oklahoma, OK 73069, USA*
[2] *Department of Physics and Astronomy, University of California at Riverside, CA 92521, USA*

(Dated: September 1, 2014)

We investigate the effect of electron-electron interactions in ABC stacked graphene trilayers. In the gapless regime, we show that the self-energy corrections lead to the renormalization of the of dynamical exponent $z = 3 + \alpha_1/N$, with $\alpha_1 \approx 0.52$ and N is the number of fermionic species. Although the quasiparticle residue is suppressed near the neutrality point, the lifetime has a sublinear scaling with the energy and the quasiparticles are well defined even at zero energy. We calculate the renormalization of a variety of physical observables, which can be directly measured in experiments.

PACS numbers: 71.10.-w, 71.10.Pm, 73.20.At

Introduction. In graphene single layers, the honeycomb arrangement of the carbon atoms leads to a linear electronic dispersion and to quasiparticles that behave as massless Dirac fermions, akin to massless neutrinos in quantum electrodynamics (QED) [1, 2]. In graphene multilayers, the electronic spectrum varies depending on the stacking sequence. In the single particle picture, rombohedral ABC-stacked trilayer graphene reveals a gapless band structure of chiral quasiparticles with Berry phase 3π and *cubic* low energy excitation spectrum [3, 4]. Because of the scaling of the kinetic energy, Coulomb interactions are relevant operators in the renormalization group (RG) sense, and can strongly renormalize different physical quantities. Different spontaneous broken symmetry ground states have been already proposed for trilayer graphene [5–7]. Very recently, transport experiments revealed a robust many-body gap of ∼40 meV at temperatures below $T_c \sim 34$K [8].

In this letter we study the effect of Coulomb interactions and polarization effects on the behavior of the quasiparticles at small but finite temperature, when the many-body gap is zero. We investigate the analytical structure of the polarization bubble and the leading self-energy corrections due to *dynamically* screened Coulomb interactions. In the gapless regime, we show that the dynamical critical exponent is renormalized to

$$z = 3 + \alpha_1/N + O(N^{-2}),$$

where $\alpha_1 \approx 0.52$ and $N = 4$ is the number of fermionic flavors. Although the quasiparticle residue is suppressed by interactions, the scattering rate has a sublinear scaling with energy and the quasiparticles remain well defined. We predict the renormalization of several physical observables in the metallic phase, such as the electronic compressibility, the specific heat, the density of states (DOS) and the spectral function, which can be measured with angle resolved photoemission (ARPES) experiments.

Low energy Hamiltonian. We start with a simplified two-band model where the high energy bands are separated in energy by interlayer hopping processes, which set the ultraviolet cut-off for the excitations in the low-energy bands, $t_\perp \sim 0.4$eV. We will assume a temperature regime above the ordering temperature $T \gtrsim T_c \sim 4$ meV, where the band structure is gapless. The infrared cut-off of the model is the trigonal warping energy ∼ 10 meV, below which the bands disperse quadratically [4].

The low energy physics of the non-interacting ABC-trilayer in the gapless regime is described by the 2×2 Hamiltonian $\mathcal{H}_0 = \sum_{\mathbf{p}} \Psi^\dagger_{\mathbf{p}} \hat{\mathcal{H}}_0(\mathbf{p}) \Psi_{\mathbf{p}}$, where $\Psi_{\mathbf{k}} = (a_{,\mathbf{k}}, \bar{b}_{,\mathbf{k}})$ is a two component spinor defined in terms of one annihilation operator in sublattice A of the top layer ($a_{\mathbf{p}}$) and another in sublattice B for the bottom layer ($\bar{b}_{\mathbf{p}}$). The total degeneracy is $N = 4$, including spin and valley degrees of freedom. The Hamiltonian density operator is [3, 4]

$$\hat{\mathcal{H}}_0 = \frac{(\hbar v)^3}{t_\perp^2} \begin{pmatrix} 0 & (\pi)^3 \\ (\pi^\dagger)^3 & 0 \end{pmatrix}, \tag{1}$$

where $\hbar v \approx 6$ eVÅ is the Fermi velocity, and $\pi = p_x - i p_y$ is defined by the x and y components of the in-plane momentum of the quasiparticles measured away from the neutrality point. In a more compact notation, $\hat{\mathcal{H}}_0(\mathbf{k}) = \gamma |\mathbf{k}|^3 \hat{h}_0(\mathbf{k})$ with

$$\hat{h}_0(\mathbf{k}) = \cos(3\theta_{\mathbf{k}})\sigma^1 + \sin(3\theta_{\mathbf{k}})\sigma^2, \tag{2}$$

where σ^i $(i = 1, 2)$ are x, y Pauli spin matrices, and $\tan\theta_{\mathbf{k}} = k_y/k_x$. The constant $\gamma \equiv (\hbar v)^3/t_\perp^2$, is proportional to the velocity of the quasiparticles $\mathbf{v}_0 = \partial_{\mathbf{k}} E_{\mathbf{k}}$, which have the energy spectrum $\pm E_{\mathbf{k}} = \pm\gamma |\mathbf{k}|^3$.

In ABC trilayers, Coulomb interactions are relevant in the RG flow at the tree level, and hence standard perturbation theory is not possible. We organize the expansion of the self-energy corrections in powers of the dynamically screened Coulomb interaction, which can be rigorously justified in the large N limit. At long wavelengths, $k \ll 1/d$, where $d \sim 2.4$Å is the interlayer distance, the bare Coulomb interaction is

$$\mathcal{H}_I = \frac{1}{2} \sum_{\mathbf{q}} V(q) \hat{n}(\mathbf{q}) \hat{n}(-\mathbf{q}), \tag{3}$$

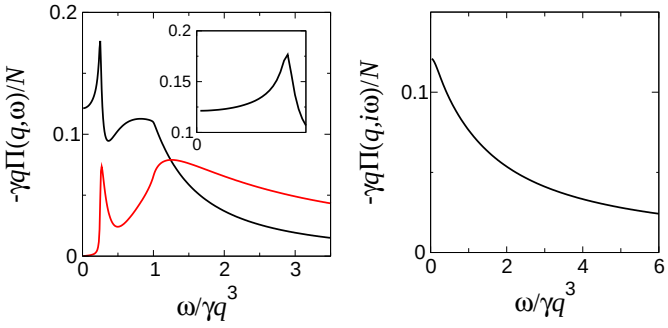

FIG. 1. Left: Polarization bubble in one loop calculated numerically from Eq. (7). The real part (black curve) has a logarithmic singularity at the edge of the particle-hole continuum, at $\omega = \gamma q^3/4$, shown in detail in the inset. Red curve: imaginary part. Right panel: Polarization in imaginary frequencies, which is a purely real function. For $\omega/\gamma q^3 \gg 1$, $\Pi^{(0)}(q, i\omega) \to -3Nq^2/(16\omega)$ (see text).

with $\hat{n}(\mathbf{q})$ a density operator and $V(q) \approx 2\pi e^2/q$, as in a 2D system. In the long wavelength regime where this approximation is valid, the DOS scales as $\rho(\mathbf{q}) = (6\pi\gamma)^{-1}/q$ and the screened Coulomb interaction is $\tilde{V}(q,\omega) = V(q)/\left[1 - V(q)\Pi(\mathbf{q},\omega)\right]$, where $\Pi(\mathbf{q},\omega)$ is the dynamical polarization function. In trilayers, the large N approximation becomes asymptotically exact at small momentum, where the DOS diverges and screening becomes strong.

Polarization bubble. In order to address the screening effects, we consider the bare polarization function, which is defined as $\Pi^{(0)}(\mathbf{q},\omega) = \frac{1}{\beta}\mathrm{tr}\sum_{i\nu}\sum_{\mathbf{p}}\hat{G}_0(\mathbf{p}, i\nu)\hat{G}_0(\mathbf{p}+\mathbf{q}, i\omega + i\nu)$, where

$$\hat{G}_0(\mathbf{q}, i\omega) = \frac{1}{2}\sum_{s=\pm}\frac{1 + s\hat{h}_0(\mathbf{q})}{i\omega - s\gamma q^3} \tag{4}$$

is the fermionic Greens function, described by a 2×2 matrix. After performing the sums over the Matsubara frequencies, the polarization function is given by

$$\Pi^{(0)}(\mathbf{q},\omega) = -\frac{N}{2}\int\frac{d^2p}{(2\pi)^2}\sum_{s=\pm}\frac{1-\cos(3\theta_{\mathbf{pq}})}{E_{\mathbf{p}+\mathbf{q}} + E_{\mathbf{p}} - s\omega} \tag{5}$$

where $\theta_{\mathbf{pq}} = \theta_{\mathbf{p}+\mathbf{q}} - \theta_{\mathbf{p}}$ is the angle between vectors $\mathbf{p}+\mathbf{q}$ and $\mathbf{p}$. By sending the ultraviolet cut-off to infinity, a simple dimensional analysis reveals the functional form of the polarization function to be $\gamma q\Pi^{(0)}(\mathbf{q}, i\omega) = -Nf(i\omega/(\gamma q^3))$. After some algebra, the scaling function $f(z)$ can be written in the form

$$f(iz) = \frac{1}{2}\int_0^{2\pi}\mathrm{d}\theta\int_0^{\infty}\frac{\mathrm{d}x\, x}{(2\pi)^2}\sum_{s=\pm}\frac{s}{iz + s\left[x^3 + h^3(x,\theta)\right]} \times\left[1 - 4\left(\frac{1+x\cos\theta}{h(x,\theta)}\right)^3 + 3\left(\frac{1+x\cos\theta}{h(x,\theta)}\right)\right], \tag{6}$$

where $z = \omega/(\gamma q^3)$ and $h(x,\theta) \equiv \sqrt{1 + x^2 + 2x\cos\theta}$. $f(z)$ is a well-defined function in imaginary frequency but has branch cuts related to the edge of the particle-hole continuum on the real axis. Due to the cubic dispersion, it is difficult to come up with a closed form solution for the polarization function. However the analytical structure of $f(z)$ near the particle-hole threshold $z = 1/4$ can be extracted in the collinear scattering approximation, which dominates the processes near that region [10]. We consider the singular contribution of the integrand around the momenta $\mathbf{p} + \mathbf{q} \approx -\mathbf{p}$. Within this window it is safe to assume $1 - \cos(3\theta_{\mathbf{pq}}) \approx 2$. After expanding $\cos\theta$ around $\theta = \pi$ to the second order, we arrive at the following integral representation for $f(z)$,

$$f(z) \cong \int\frac{xdx}{(2\pi)^2}\int\frac{d\theta}{x^3 + (1-x)^3 + \frac{3}{2}x(1-x)\theta^2 - z}. \tag{7}$$

Considering the rapid fall of the integrand with respect to θ around π, one can conveniently extend the upper limit of the angular integral to infinity, $\theta \in [0, \infty[$. After performing the integrals, we arrive at the most dominant part of $f(z)$ near $z \sim 1/4$,

$$f(z) = -\frac{1}{6\sqrt{2}\pi}\ln\left(1 - 4|z|\right) + \text{regular terms}, \tag{8}$$

which describes a logarithmic divergence near the edge of the particle hole continuum. Exploring the two asymptotic regimes, in the $z \to 0$ regime, $f(0) = c_0 \approx 0.12$ is a constant [11, 12] and in the $z \gg 1$ limit, $f(z) \to -ic_\infty/z$ is purely imaginary, with $c_\infty = 3/16$.

In Fig. 1, we show the behavior of the real and imaginary parts of $f(z)$ calculated numerically from Eq. (7). The scaling function has only one singularity near $z \sim 1/4$. For $z < 1/4$, $f(z)$ is purely real and diverges logarithmically at $z = 1/4$, in agreement with the analytical expression (8), as shown in the inset of Fig. 1. For $z > 1/4$, $f(z)$ has also an imaginary part, which decays with $1/z$. The right panel of Fig. 1 shows $f(iz)$ in imaginary frequency, which is a real and well behaved monotonic function.

In the optical regime, for $z \gg 1$, where $\Pi^{(0)}(q,\omega) \to iNc_\infty q^2/\omega$, the optical conductivity can be calculated directly from the charge polarization,

$$\sigma(\omega) = \frac{e^2}{\hbar}\lim_{q\to 0}\frac{i\omega}{q^2}\frac{\Pi^{(0)}(\mathbf{q},\omega)}{1 - V(q)\Pi^{(0)}(\mathbf{q},\omega)} = \frac{3}{4}\frac{e^2}{\hbar}, \tag{9}$$

which is proportional to the Berry phase 3π. In the general case, $\sigma(\omega) = \nu e^2/(2h)$, with $\nu = \pi$ for graphene single layer and $\nu = 2\pi$ for bilayers.

Self-energy. The leading self energy correction due to the screened Coulomb interaction is diagrammatically shown in Fig. 2. In imaginary time, the self-energy is

given by

$$\hat{\Sigma}^{(1)}(\mathbf{q}, i\omega) = -\frac{1}{\beta}\sum_{\nu}\int\frac{\mathrm{d}^2p}{(2\pi)^2}\tilde{V}(\mathbf{p}, i\nu)\hat{G}^{(0)}(\mathbf{q}-\mathbf{p}, i\omega - i\nu). \tag{10}$$

Through power counting, the leading divergences appear at long wavelengths, where the large N limit is a good approximation. At large N, the dynamically screened potential is approximated by $\tilde{V}(\mathbf{q}, i\omega) \approx \gamma q/[Nf(i\omega/\gamma q^3)] + O(N^{-2})$ [14–16]. Since $f(iz)$ is a well behaved function, with no singularities or branch cuts, the self energy in one loop can be calculated directly in the zero temperature limit. The leading contribution is logarithmically divergent,

$$\Sigma^{(1)}(\mathbf{q}, i\omega) = \frac{1}{2\pi^2 N}\left[\alpha_d i\omega + \alpha_o\gamma q^3\hat{h}(\mathbf{q})\right]\ln\left(\frac{\Lambda}{q}\right), \tag{11}$$

where $t_\perp = \gamma\Lambda^3$ defines the ultraviolet cut-off in momentum, namely $\Lambda = t_\perp/(\hbar v)$. The coefficients

$$\alpha_o = \int_0^\infty dz \frac{1}{f(iz)}\frac{z^2(10 - 16z^2 + z^4)}{(1+z^2)^4}, \tag{12}$$

and

$$\alpha_d = \int_0^\infty dz \frac{1}{f(iz)}\frac{1 - z^2}{(1+z^2)^2}, \tag{13}$$

can be found though numerical integration using the exact $f(iz)$ from Eq. (7). Although α_o and α_d both diverge logarithmically with the upper limit of integration at large z, we will postpone their regularization for the moment, since these divergences cancel exactly in the renormalization of γ and hence have no consequence to the renormalization of the spectrum.

The self-energy can be separated in two terms, $\hat{\Sigma}(\mathbf{q}, i\omega) = i\omega\Sigma_d\sigma_0 + \Sigma_0 q^3\hat{h}_0(\mathbf{q})$, where Σ_d is the diagonal term, and Σ_o describes the off-diagonal matrix elements. The diagonal part of the self-energy has frequency dependence and defines the quasiparticle residue renormalization,

$$Z_\psi^{-1} = 1 - \partial\hat{\Sigma}/\partial(i\omega) = 1 - \Sigma_d. \tag{14}$$

The renormalized Green's function is $\hat{G}(\mathbf{q}, i\omega) = Z_\psi[i\omega - \gamma\hat{h}_0(\mathbf{q})Z_\psi(1+\Sigma_o)]^{-1}$. In one loop, the renormalized energy spectrum is

$$\frac{\gamma(q)}{\gamma} = \frac{1+\Sigma_o}{1-\Sigma_d} \approx 1 - \frac{\alpha_1}{N}\ln\left(\frac{\Lambda}{q}\right) + O(1/N^2), \tag{15}$$

where

$$\alpha_1 = \frac{\alpha_0 + \alpha_d}{2\pi^2} = \int_0^\infty \frac{\mathrm{d}z}{2\pi^2}\frac{1}{f(iz)}\frac{17z^4 - 11z^2 - 1}{(1+z^2)^4} \approx 0.52 \tag{16}$$

is a finite well defined quantity.

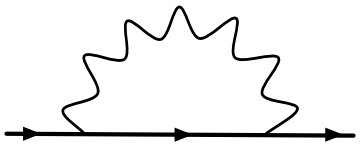

FIG. 2. One-loop correction to the self-energy with the dressed Coulomb interaction.

The logarithmic renormalization of the quasiparticle velocity in one loop dictates the RG equation of γ,

$$\beta_\gamma \equiv \frac{\mathrm{d}\gamma}{\mathrm{d}l} = -\gamma\frac{\alpha_1}{N}, \tag{17}$$

where $l = \ln(\Lambda/\Lambda')$, with $\Lambda' < \Lambda$ the renormalized cut-off, whose solution is

$$\gamma(q) = \gamma \times [(\hbar v/t_\perp)q]^{\alpha_1/N}. \tag{18}$$

The energy spectrum acquires an anomalous dimension $\eta = \alpha_1/N$, which leads to the renormalization of the dynamical exponent, $\omega \propto q^z$, with $z = 3 + \alpha_1/N + O(N^{-2})$. This result can be related with the graphene bilayer case, where $\eta = 0.078/N$ [17] and with the large N limit of the single layer case, where $\eta = -4/(\pi^2 N)$ [14, 15].

This analysis can be explicitly verified by checking the two loop correction in the self energy. The RG equation describes a resummation of leading logs to all orders in $1/N$. The $N^{-2}\log^2$ terms cancel exactly in the vertex correction diagram at two loop, and hence vertex corrections do not renormalize in the RG flow [17]. The leading logarithmic terms appear in the remaining diagrams of the same order, and lead to a second order correction to Eq. (15), $\gamma^{(2)}(q)/q = \frac{1}{2}\alpha_1^2/N^2\ln^2(\Lambda/q)$, in agreement with the result of the RG equation up to $1/N^2$ order.

Quasiparticle residue. To calculate the quasiparticle residue renormalization Z_ψ through Eq. (14), one needs to regularize integral (13). That can be done introducing an upper cut-off z_c which accounts for the condition where the large N limit breaks down, namely $-V(p)\Pi^{(0)}(p, ip) = 2\pi N e^2\Lambda^2/(\hbar v p^2) f(iz_c) \sim 1$. At large z, where $f(iz) \to 3/(16z)$, the leading contribution is $\alpha_d \sim -16\ln(\Lambda/p)$. Replacing $\ln(\Lambda/q) \to \int_q^\Lambda \mathrm{d}p/p$ in Eq. (11) and carrying out the momentum integration, the quasiparticle residue Z_ψ is given by

$$Z_\psi^{-1} \to 1 + \frac{4}{\pi^2 N}\ln^2(\Lambda/q) + O(1/N^2), \tag{19}$$

in one loop, and is suppressed logarithmically in the infrared.

In the RG spirit, we now reestablish the bare value of the quasiparticle residue Z_0 in the bare Green's function $\hat{G}_0 \propto Z_0$ [18], and set $Z_0 \to 1$ at the end. Since $\delta\hat{G} = \hat{G}_0\hat{\Sigma}\hat{G}_0 \propto \delta Z_\psi$ in lowest order in the Dyson equation, then $\delta Z_\psi = Z_0^2\hat{\Sigma}_d \propto Z_0$ in large N. Eq. (19)

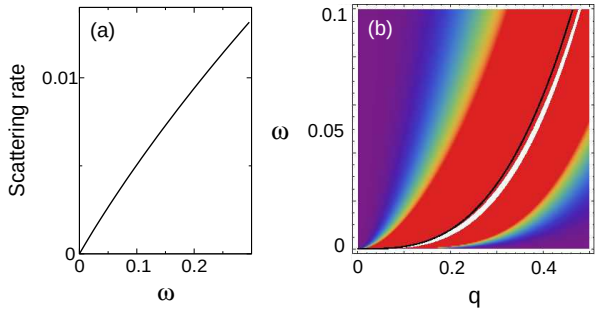

FIG. 3. a) On-shell scattering rate $\tau(\omega)$ vs energy in units of $t_\perp \sim 0.4$eV. b) Density plot of the spectral function as a function of energy $(\omega/t_\perp)$ and momentum (q/Λ). Solid black line: bare energy spectrum. White line: renormalized one. Light regions indicate higher intensity.

then becomes $\delta Z_\psi = -4Z_0/(\pi^2 N)\delta \ln^2(\Lambda/q)$, which corresponds to the RG equation

$$\beta_\psi = \frac{\mathrm{d}Z_\psi}{\mathrm{d}l} = -\frac{8}{\pi^2 N} l Z_\psi, \tag{20}$$

with $l = \ln(\Lambda/\Lambda')$, whose solution is

$$Z_\psi(q) = \exp\left[-4/(\pi^2 N)\ln^2(\Lambda/q)\right], \tag{21}$$

in agreement with Eq. (19) up to $1/N$ order.

Quasiparticle lifetime. In real frequency, the polarization function has a logarithmic branch cut. To calculate the quasiparticle scattering rate $\tau = Z_\psi \mathrm{Im}\hat{\Sigma}$, we use the method in ref. [19] to separate the self-energy into the line part and the residue part, $\hat{\Sigma} = \hat{\Sigma}_{\mathrm{line}} + \hat{\Sigma}_{\mathrm{res}}$. The line part is obtained by performing Wick rotation $i\omega \to \omega + i0_+$ in the self-energy (10), and is purely real. The residue part follows from the residue calculated around the pole of the Green's function,

$$\Sigma^{(1)}_{\mathrm{res}}(\mathbf{q},\omega) = -\frac{1}{2}\sum_{s=\pm}\int \frac{\mathrm{d}^2 p}{(2\pi)^2}\tilde{V}(|\mathbf{q}|,\omega)[1+s\hat{h}(\mathbf{q}-\mathbf{p})] \times [\theta(\omega - s\gamma|\mathbf{q}-\mathbf{p}|^3) - \theta(-s\gamma|\mathbf{q}-\mathbf{p}|^3)], \tag{22}$$

with θ a step function. The scattering rate is given by $\tau(\mathbf{q},\omega) = Z_\psi \mathrm{Im}\Sigma_{\mathrm{res}}(\mathbf{q},\omega)$. In the on-shell region, near $\omega \sim \gamma q^3$, $\tau(\omega) = \omega Z_\psi g(\omega/t_\perp)$, where

$$g(y) = \frac{1}{2N}\,\mathrm{Im}\int_{|\mathbf{x}|<1}\frac{\mathrm{d}^2 x}{(2\pi)^2}\frac{|\hat{q}-\mathbf{x}|}{\bar{\alpha}y^{2/3}|\hat{q}-\mathbf{x}|^2 + f\left(\frac{1-x^3}{|\hat{q}-\mathbf{x}^3|}\right)} \tag{23}$$

is a scaling function in one loop, with $y = \omega/t_\perp$, $\bar{\alpha} = \hbar v/(2\pi N e^2)$ is a dimensionless constant and $\hat{q} = \mathbf{q}/q$. The function $g(y)$ has a very slow variation, as shown in Fig. 3a, and as a consequence $\tau(\omega) \sim \omega Z_\psi[(\omega/\gamma)^{1/3}]$ has a sublinear scaling with energy within logarithmic accuracy. In the large N limit ($\bar{\alpha} \to 0$), which is valid at low energy, $g(y) \approx 0.043$ is a constant. Since the ratio $\tau(\omega)/\omega \ll 1$, the quasiparticles are well defined even in the $\omega \to 0$ limit.

The spectral function is given by $A(\mathbf{q},\omega) = -2\mathrm{tr}\,\mathrm{Im}G^R(\mathbf{q},\omega)$, where

$$\hat{G}^R(\mathbf{q},\omega) = \frac{1}{2}\sum_{s=\pm}\frac{Z_\psi(q)[1+s\hat{h}_0(\mathbf{q})]}{\omega - s\gamma(q)q^3 - i\tau(\omega) + i0^+} \tag{24}$$

is the retarded part of the renormalized Green's function. The spectral function is shown in Fig. 3b. The solid black line describes the bare energy spectrum, while the light region describes the renormalized one, which corresponds to the pole of the renormalized Green's function. There is a clear deviation of the two curves, which could be observed with ARPES experiments.

Other physical observables. The renormalization of the quasiparticle velocity encoded in the RG flow of γ leads to the renormalization of many physical observables. For instance, the specific heat for non-interacting particles with cubic dispersion in 2D scales with $C \sim (T/\gamma)^{2/3}$, where T is the temperature. From Eq. (18), the scaling of γ with energy is $\gamma \sim \omega^{\alpha_1/(3N)}$. At $\omega \sim T$, the temperature scaling of the specific heat is renormalized to

$$C \sim T^{2(1-\alpha_1/(3N))/3} \approx T^{2/3-0.1/N}, \tag{25}$$

neglecting slower logarithmic corrections due to the scaling of Z_ψ, with $T \gtrsim T_0$, where T_0 is defined by the infrared energy cut-off of 10meV due to trigonal warping effects [4]. In the same way, the renormalized DOS is $\rho(q) = [6\pi\gamma(q)]^{-1}/q \sim q^{-(1+\alpha_1/N)}$, which can be measured directly on surfaces with scanning tunneling spectroscopy experiments [20, 21].

In 2D systems, the electronic compressibility can be characterized with single electron transistor measurements [22]. By dimensional analysis, the free electronic compressibility scales with temperature as $\kappa \sim \gamma^{-2/3}T^{-1/3}$ [23]. In the same spirit, interactions renormalize the scaling of the inverse compressibility,

$$\kappa^{-1} \sim T^{[1+2\alpha_1/(3N)]/3} \approx T^{1/3+0.1/N}, \tag{26}$$

which strongly deviates from the non-interacting result.

In summary, we derived the effect of electron-electron interactions in the renormalization of a variety of different physical observables in the metallic phase of ABC graphene trilayers.

We thank F. Guinea, V. N. Kotov and K. Mullen for valuable discussions. B. U. acknowledges University of Oklahoma and NSF grant DMR-1352604 for partial support.

[1] A. H. Castro Neto, N. M. R. Peres, F. Guinea, K. Novoselov, A. K. Geim, Rev. Mod. Phys. **81**, 109 (2009).

[2] V. N . Kotov, B. Uchoa, V. M. Pereira, F. Guinea, A. H. Casto Neto, Rev. Mod. Phys. **84**, 1067 (2012).

[3] F. Guinea, A. H. Castro Neto, N. M. R. Peres, Phys. Rev. B **73**, 245426 (2006).

[4] F. Zhang, B. Sahu, H. Min, and A. H. MacDonald, Phys. Rev. B **82**, 035409 (2010).

[5] V. Cvetkovic, and O. Vafek, arXiv:1210.4923v1 (2012).

[6] J. Jia, E. V. Gorbar, and V. P. Gusynin, Phys. Rev. B **88**, 205428 (2013).

[7] R. Olsen, R. van Gelderen, and C. Morais Smith, Phys. Rev. B **87**, 115414 (2013).

[8] Y. Lee, D. Tran, K. Myhro, J. Velasco Jr., N. Gillgren, C. N. Lau, Y. Barlas, J.M. Poumirol, D. Smirnov, F. Guinea, arXiv:1402.6413.

[9] Y. Barlas, and K. Yang, Phys. Rev. **B** 80, 161408 (2009).

[10] S. Gangadharaiah, A. M. Farid, E. G. Mishchenko, Phys. Rev. Lett. **100**, 166802 (2008).

[11] H. Min, E. H. Hwang, S. Das Sarma, Phys. Rev. B **86**, 081402(R) (2012).

[12] R. van Gelderen, R. Olsen, C. Morais Smith, Phys. Rev. B **88**, 115414 (2013).

[13] M. G. Menezes, R. B. Capaz, S. G. Louie, Phys. Rev. B **89**, 035431 (2014).

[14] D. T. Son, Phys. Rev. B **75**, 235423 (2007).

[15] M. S. Foster, I. L. Aleiner, Phys. Rev. B **77**, 195413 (2008).

[16] V. N. Kotov, B. Uchoa, A. H. Castro Neto, Phys. Rev. B **80**, 165424 (2009).

[17] Y. Lemonik, I. L. Aleiner, C. Toke, V. I. Fal'ko, Phys. Rev. B **82**, 201408(R) (2010).

[18] R. Nandkishore, L. Levitov, Phys. Rev. B **82**, 115431 (2010).

[19] J. J. Quinn and R. A. Ferrell, Phys. Rev. **112**, 812 (1958).

[20] G. Li, A. Luican, E. Y. Andrei, Phys. Rev. Lett. **102**, 176804 (2009).

[21] M. Yankowitz, J. I.-J. Wang, A. G. Birdwell, Y.-A. Chen, K. Watanabe, T. Taniguchi, P. Jacquod, P. San-Jose, P. J.-Herrero, B. J. LeRoy, Nat. Materials **13**, 786 (2014).

[22] J. Martin, N. Akerman, G. Ulbricht, T. Lohmann, J. H. Smet, K. Von Kliyzin, A. Yacoby, Nat. Phys. **4**, 144 (2008).

[23] G. D. Mahan, Many particle Physics, (Plenum, New York, third edition).